Tomato-Like Shaped PVP - Capped PbS Thin Film Chemically Deposited by CBD

Chidimma G. Ezema[1] *, Solomom U. Offiah[1], Pius O. Ukoha[2], Benjamin E. Ezema[2] and   Fabian I. Ezema[3]

[1]National Centre for Energy Research & Development, University of Nigeria, Nsukka, Enugu State, Nigeria.
[2]Department of Pure and Industrial Chemistry, University of Nigeria, Nsukka, Enugu State, Nigeria.
[3]Department of Physics and Astronomy, University of Nigeria, Nsukka, Enugu State, Nigeria.

*Corresponding author: chidimmaokpara@yahoo.com, +2348037587724

Abstract

Lead sulphide thin films were deposited on glass substrates using solution method. The films were deposited at ambient temperature using lead acetates, thiourea and sodium hydroxide in polyvinyl pyrrolidon (PVP). The as-deposited films appeared greyish in colour, with uniform deposits adherent to the substrate. The as-deposited and annealed films were characterized for structural, morphological, compositional, and optical properties. The X-ray diffraction (XRD) studies revealed that the annealed films are polycrystalline in nature with cubic phases. The energy dispersive analysis by X-ray (EDAX) showed that the films were rich in lead. The surface morphologies of the thin films were determined by scanning electron microscope measurements. The optical studies were carried out from spectroscopy measurements in the wavelength range 200-1100 nm. The range of the estimated optical band gap energy is 1.35eV – 1.55eV.

Keywords: PbS, chemical deposition, thin film, annealing, PVP

1. INTRODUCTION

Semiconductor materials are always in focus due to their outstanding electronic and optical properties and potential applications in various devices. The electronic and optical properties of semiconductor materials can be changed by changing their size and shapes [1]. Therefore, the optimization of synthesis parameters of these nanoparticles is important in order to improve their properties. The fabrication technique of nanoscale materials with controlled shape and high dispersion using polymeric or other conventional capping materials is known as capping assisted chemical bath deposition (CACBD) technique. As an important IV-VI group semiconductor, lead sulphide (PbS) is a direct narrow band gap semiconductor material of ≈ 0.41 eV at room temperature [2] and has a relatively large excitation Bohr radius of 18 nm [3] making it an interesting material to study the quantum effects over the wide range of particle size [4]. Quantum size effects are usually characteristic of nanocrystallites measuring less than 10 nm. This property makes it an excellent candidate for opto-electronic applications in many fields such as photography, IR detectors, solar absorbers, light emitting devices and solar cells [5,6,7,8,9].

Hence, there has been growing interest in developing techniques for preparing semiconductor nanoparticle films. These materials can be obtained in thin film form by various methods, including chemical bath deposition [10], electrodeposition [11], and microwave heating [12]. The chemical bath deposition is simple, economical and convenient for large area deposition of IV-VI compounds.

However, the conventional processes usually produce particles with large size, and irregular shape and aggregation. The use of polymer protection like PVP has been found to regulate the pattern of arrangement of particle. Zongtao, Zhang and Hu [13] have reported a PVP protective mechanism of ultrafine silver powder synthesized by chemical reduction processes in which PVP as a protective agent plays a decisive part in controlling superfine silver particle size and size distribution by reducing silver nitrate with hydrazine hydrate. A newly developed chemical method, known as the polymer protected reduction process, has been used to prepare monodispersed silver powder with submicrometer size and quasi-spherical shape [14, 15]. G. Tosun and H. D. Glichsman [16] have also reported a gelatin protected processing, which was similar to that of PVP. F. Fievet *et al.* [14] and Ducamp-Sanguesa *et al.* [15] have employed polyvinyl pyrrolidone(PVP) as a protective agent to synthesize ultrafine silver powder with 300 nm diameter, by reducing silver nitrate with hot polyol solution.

Proceedings of the 1st African International Conference/Workshop on Applications of Nanotechnology to Energy, Health and Environment, UNN, March 23 – 29, 2014

Page 76

Polymer protective mechanisms originated from colloidal chemistry. H. Hirai *et al.* [17] suggested that a complex of the polymers and the metal ions was formed. According to chemical equilibrium, the effective metal ion concentration decreased, so the polymer had impaired the metal ion reduction, i.e., the nucleation of metal particles, the coordinative bonds between the polymers and the ions being too strong. On the other hand, the polymers usually have the back bone of polyvinyl as hydrophobic and hydrophilic groups. The backbone of the vinyl polymer forms a hydrophobic domain, which surrounds metal particles, whereas the hydrophilic pendant groups of the polymer interact with water or polar solvent, i.e., the steric effect of the polymer in the surface of metal particles prevents the particles from agglomeration.

Numerous inorganic/organic polymer composite nanofibers have been prepared by electrospinning method. Wang and co-workers [18-21] have successfully formed composite nanofibers of metal sulfide nanoparticles and polymer nanofibers, such as PbS/poly(vinyl pyrrolidone) (PVP), CdS/PVP, Ag$_2$S/PVP and Ag$_2$S/polyacrylonitrile (PAN). In their studies, the metal salt/polymer nanofibers were obtained via electrospinning method, and then the metal nanoparticles were formed in the nanofibers via gas–solid reaction of metal ion and gaseous H$_2$S.

This paper reports on investigations of structural, morphological and optical properties of nanocrystalline PbS/PVP- based nanofibers by chemical bath deposition technique.
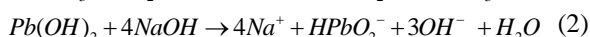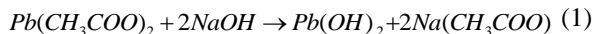
2. EXPERIMENTAL

All the chemicals used for the deposition were analytical grade and all the solutions were prepared in distilled water. Glass slides of dimension, $35 \times 20 \times 1.35$ mm^3, were used as substrates. They were suitably cleaned in detergent, sulphuric acid and distilled water, rinsed in ethanol, acetone, and distilled water and dried in an oven. To obtain PbS polycrystalline thin films onto the glass slides, precursors for the PbS thin film bath is shown in Table 1.
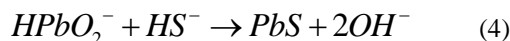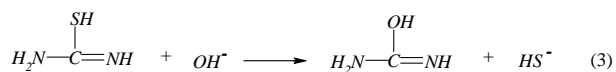
Table 1: Precursors for the PbS thin film bath

PRECURSORS	CONCENTRATION	VOLUME
Lead acetate [Pb(CH$_3$OO)$_2$]	0.05M	15 ml
Thiourea [(NH$_2$)$_2$SC]	0.10M	15 ml
PVP [(C$_6$H$_9$NO)n]		30 ml
Sodium hydroxide (NaOH)	1.00M	5 ml

The reagents were added according to the order into a beaker. The pH of the solution was adjusted to 11 with the NaOH. The previously prepared substrates were vertically suspended into the beaker. The deposition was achieved after 45 minutes at room temperature. Subsequently, the substrates were taken out of the bath, rinsed with distilled water, dried and preserved in a dust free container. The possible reaction process in solution is suggested via the following reactions:

$$Pb(CH_3COO)_2 + 2NaOH \rightarrow Pb(OH)_2 + 2Na(CH_3COO) \quad (1)$$

$$Pb(OH)_2 + 4NaOH \rightarrow 4Na^+ + HPbO_2^- + 3OH^- + H_2O \quad (2)$$

In alkaline medium, thiourea decomposes and releases S^{2-} ions which precipitates Pb^{2+} ions from solution.

$$H_2N-\overset{\overset{SH}{|}}{C}=NH \; + \; OH^- \longrightarrow H_2N-\overset{\overset{OH}{|}}{C}=NH \; + \; HS^- \quad (3)$$

$$HPbO_2^- + HS^- \rightarrow PbS + 2OH^- \quad (4)$$

Deposition of the films from a solution involves a nucleation phase in which an initial layer of Pb(OH)$_2$, formed on the glass substrate, is chemically converted into PbS by the reaction with S^{2-} ions available in the bath from the hydrolysis of thiourea. The presence of Pb(OH)$_2$ in the as-prepared bath is very vital for the deposition of PbS thin films. The precipitation of metal chalcogenides in CBD occurs only when the ionic product exceeds the solubility product of metal chalcogenides i.e. PbS. The film growth takes place via ion-by-ion condensation of the materials or by adsorption of colloidal particles from the solution onto the substrate.

The samples of the PbS thin films were labeled 31a, 31b, 31c, 31d and 31e. While 31a was left as-grown, the rest were respectively annealed at 100 ℃, 200 ℃, 300 ℃ and 400 ℃.

X-ray diffraction studies were carried out on all the samples using X'Pert HighScore PW1710 PANanalytical diffractometer in the scanning range of 2θ from $10° – 80°$ with Cu-kα ($\lambda = 1.5406$ Å) radiations. The surface morphology and composition was studied by scanning electron microscopy (SEM) and energy dispersive analysis by X-ray (EDAX) with the help of JEOL-JSM 5600 Japan. The optical absorption studies were carried out using UV-VIS-NIR spectrophotometer (Unico- UV- 2102PC Japan) in the 200-1000 nm wavelength range.

3. RESULTS AND DISCUSSION

3.1. Structural Analysis

The XRD patterns of the PVP-capped PbS thin films are displayed in figure 1. The pattern for the as-deposited PVP-capped PbS thin films on glass substrate showed several diffraction peaks at 2θ values shown in Table 2. The un-annealed sample was amorphous and on annealing, the samples became crystalline (Figure 1). There was an increase in the size of the grain size from 7.37 to 10.07nm thermal treatments at 200ºC and 400ºC respectively. The various diffraction 2-theta angles and the corresponding preferred planes of orientation are summarized in table 2.
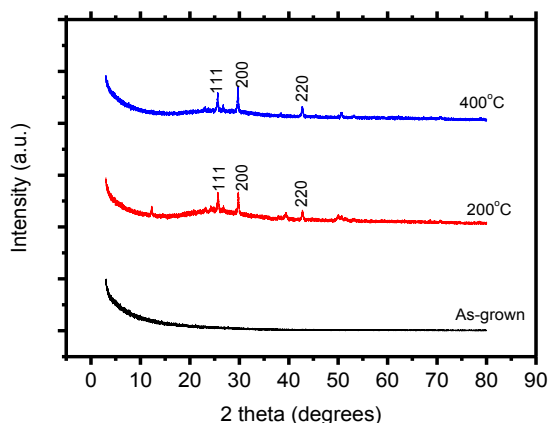

Figure 1: The XRD Patterns of the PbS (a) as grown

(b) annealed at 200ºC (c) annealed at 400ºC

The XRD patterns compare very well with the standard JCPDS cards (card no. 5-0592). The average grain sizes of the thin films were evaluated using the Scherrer's formula given by

$$D = (k \lambda) / (\beta \cos \Theta) \qquad (5)$$

where θ, β, k and λ represent the Bragg's angle, the FWHM, a constant (assumed 0.94) and the wavelength of the X-ray (1.54060 Å) respectively.

Table 2: Summary of the XRD results

Sample	As deposited	Annealed at 200°C	Annealed at 400°C
Diffraction peak angles (2θ)	Amorphous	25.71°, 29.79°, 42.76°, 53.25°	25.64°, 29.78°, 42.74°, 50.69°
Diffraction planes (h k l)	-	111, 200, 220, 222	111, 200, 220
Average grain size (nm)	-	7.37	10.07

3.2. Surface morphology and EDAX analysis

Figures 2a, 2b, and 2c, show the scanning electron micrographs of PbS thin films. It is seen that the SEM of the as deposited thin films revealed nano-rods which were coiled into flower bud-like or tomato-like structures. These flower-like particles uncurled after been annealed at different temperature revealing the PbS nano-crystalline rods. (1 – 10 μm length). This could possibly be the reason why the XRD of the annealed PbS thin films became more crystalline after the thermal treatment. The size of the PVP-capped PbS nano-rods annealed at 400ºC as seen on the SEM confirms the increase in the particle sizes as were calculated using the Scherrer's formula. Comparatively, Wang and co-workers who reported PbS nanoparticles dispersed in polymer-fiber matrices by electrospinning obtained PbS nanoparticles roughly spherical in shape, each with a diameter of approximately 5 nm, and do not aggregate [18]. X. Shi et al [22] reported great change in morphologies of products with varying PVP amounts revealing that the PVP-assisted dynamical crystal growth process was responsible for the formation of BiOBr HNs and speculate that PVP can regulate the morphology of

samples and control the thickness and distance of nanosheets. This work agrees with that speculation that PVP is responsible for the shape gotten in the as-grown and was destroyed by heat during the annealing process.
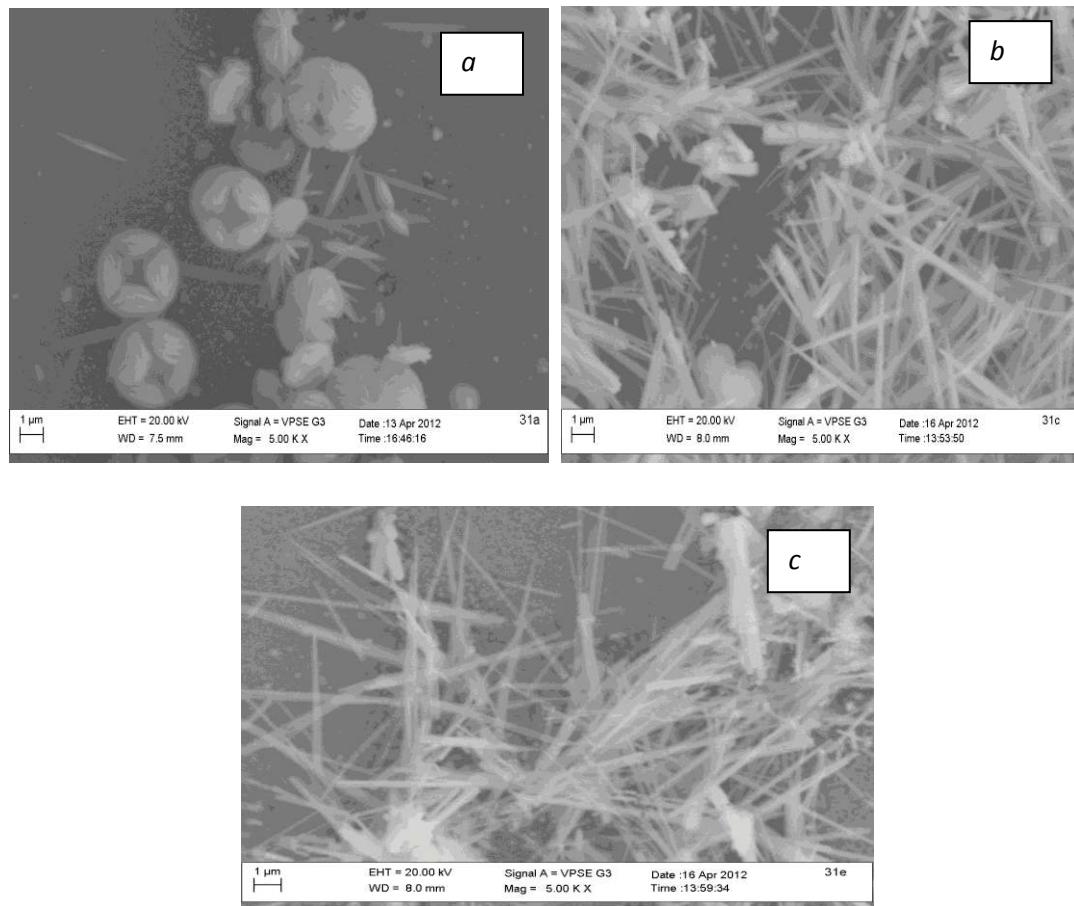

Fig 2: SEM micrograph of the PbS (a) as grown (b)annealed at 200ºC (c) annealed at 400ºC

The energy-dispersive analysis by X-ray was used to determine the composition of PbS thin film. The average elemental ratio of Pb:S calculated from the spectra were 1:1, 4:1 and 1:1 (for 31a, 31b and 31c respectively). This confirms that the films are rich in lead (Pb). Other elements seen are components of the glass substrate namely: Si, Na, K, Ca, Al, Mg and O. The possible composition and structure of chemically deposited PbS thin films can vary widely may be due to the variation of pH value.

PbS thin film exhibits direct band transition, the band gap energy obtained for the thin films are 31a (as-deposited) = 1.35 eV, 31b (100ºC) = 1.50 eV, 31c (200ºC) = 1.50 eV, 31d (300ºC) = 1.55 eV, 31e

3.3. Optical Band Gap

The band gap energy (E_g) of the deposited films were obtained by analyzing the optical data using the expression:

$$\alpha h\nu = C (h\nu - E_g)^n \qquad (6)$$

where α is optical absorbance, $h\nu$ is photon energy, C is a constant and the exponential n depends on the type of transition. Figure 3 is a plot of $(\alpha h\nu)^2$ versus photon energy ($h\nu$) of PbS thin films. The energy gaps for these films are obtained by extrapolating the linear part of the curve to the energy axis.

(400ºC)= 1.55 eV as shown in Figure 3. The values of the band gap were higher than that of bulk PbS (0.41eV), the blue shift from the near IR to the visible region is 0.94 eV, 1.09 eV, 1.09 eV, 1.14 eV, and 1.14

Proceedings of the 1st African International Conference/Workshop on Applications of Nanotechnology to Energy, Health and Environment, UNN, March 23 – 29, 2014

Page 79

eV for a, b, c, d and e respectively. Therefore, exhibit good optical and electrical properties and applications in nonlinear optical devices such as IR detectors, display devices, Pb^{2+} ion-selective sensors.
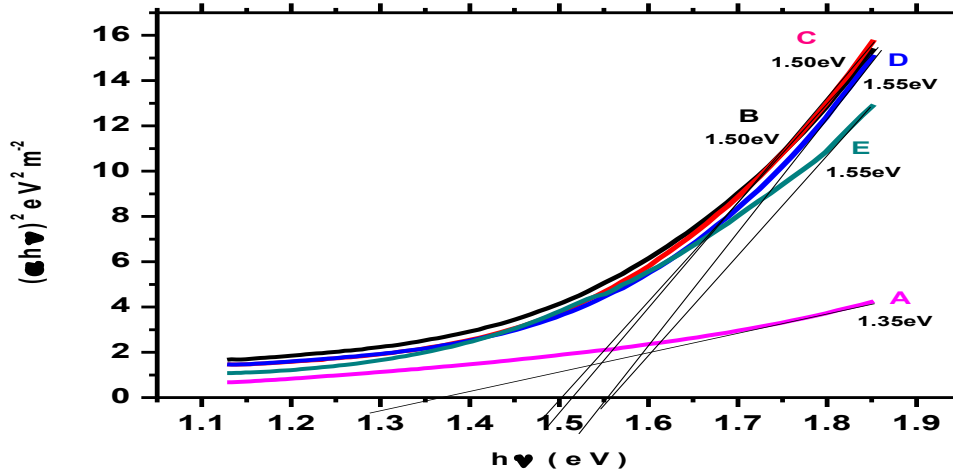

Figure 3: Figure 5: Plot of (αhv)² as a function of photon energy (hv) for the Lead sulfide thin films

3.4. Transmittance

The thin films have very low transmittance in the visible region but higher towards the near the near infra red regions. This increased from as low as 5% in the VIS region to about 40% at the NIR region of the electromagnetic spectrum as can be seen in Figure 4.
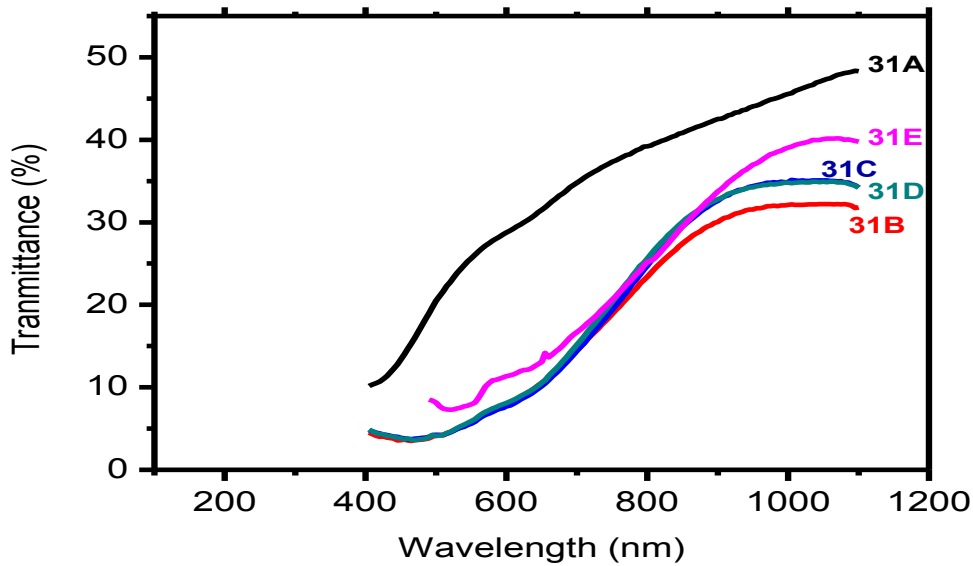

Figure 4: Plot of transmittance VS wavelength of the photons

Proceedings of the 1st African International Conference/Workshop on Applications of Nanotechnology to Energy, Health and Environment, UNN, March 23 – 29, 2014

Page 80

4. CONCLUSION

The growth of the PbS thin films on glass substrates using PVP as the deposition medium was successful. Thermal treatments improved the crystallinity of the PVP-capped PbS thin films but destroyed the shape. The SEM of the thin films revealed nano-crystalline rods of length between 1.0 and 10.0 μm. The average grain sizes were between 7.37 and 10.07nm. The variations in the transmittance of the thin films can be tailored to be used in solar thermal conversion.

REFERENCES

1. P. D. Yang, C. M. Lieber, *Science*, **273**, 1836 (1996).
2. S. Seghaier, N. Kamoun, R. Brini, A. B. Amara, *Mater. Chem. Phys.* **97**, 71 (2006).
3. J.L. Machol, F.W. Wise, R.C. Patel, D.B. Tanner, *Phys. Rev. B* **48**, 2819 (1993).
4. J. E. Murphy, M. C. Beard, A. G. Norman, S. P. Ahrenkiel, J. C. Johnson, P. Yu, O. I. Micic, R. J. Ellingson, A. J. Nozik, *J. Am. Chem. Soc.* **128**, 3241 (2006).
5. P. K. Nair, O. Gomezdaza, M. T. S. Nair, *Adv. Mater. Opt. Electron.* **1**, 139 (1992).
6. P. Gadenne, Y. Yagil, G. Deutscher, *J. Appl. Phys.* **66**, 3019 (1989).
7. T. K. Chaudhuri, S. Chatterjee, *Proc. of 11th Int. Conf. Thermoelectrics*, p. 40, Arlington, USA (1992).
8. S. A. Mcdonald, G. Konstantatos, S. Zhang, P. W. Cyr, E. J. D. Klem, L. Levina, E. H. Sargent, *Nat. Mater.* **4**, 138 (2005).
9. E. H. Sargent, *Adv. Mater.* **17**, 515 (2005).
10. Schmidt, *Chem. Rev.,* **92**, 1709 (1992).
11. N. Molin and A. Dikusar, *Thin Solid Films*, **265**, 3 (1995).
12. J. J. Zhu, O. Palchik, S.G. Chem and A. Gedanken, *J. Phys. Chem.*, **104**, 7344 (2000).
13. Zongtao Zhang, Bin Zhao, and Liming Hu. *J. of Solid State Chem.* **121**, 105–110 (1996).
14. F. Fievet, J. P. Lagier, and B. Blin, *Solid State Ionics* **32/33,** 198 (1989). In: Zongtao Zhang, Bin Zhao, and Liming Hu. *J. of Solid State Chem.* **121**, 105–110 (1996).
15. C. Ducamp-Sanguesa, R. Herrera-Orbina, and M. Figlarz, *J. Solid State Chem.* **100**, 272 (1992). In: Zongtao Zhang, Bin Zhao, and Liming Hu. *J. of Solid State Chem.* **121**, 105–110 (1996).
16. G. Tosun, and H.D. Glicjsman, U.S. Patent 4,978,985. In: Zongtao Zhang, Bin Zhao, and Liming Hu. *J. of Solid State Chem.* **121**, 105–110 (1996).
17. H. Hirai, Y. Nakao, and N. Toshima, *J. Macromol. Sci. Chem.* **A13,** 727 (1979).
18. X. Lu, Y. Zhao, C.Wang, *Adv. Mater.* **17**, 2485 (2005).
19. X.F. Lu, Y.Y. Zhao, C.Wang, Y.Wei, *Macromol. Rapid Commun.* **26**, 1325 (2005). In: Jie Bai, Yaoxian Li, Chaoqun Zhang, Xiaofei Liang, Qingbiao Yang. *Colloids and Surf. A* **329**, 165 (2008).
20. X.F. Lu, L.L. Li, W.J. Zhang, C.Wang, *Nanotechnology* **16**, 2233 (2005). In: In: Jie Bai, Yaoxian Li, Chaoqun Zhang, Xiaofei Liang, Qingbiao Yang. *Colloids and Surf. A* **329**, 165 (2008).
21. F.X. Dong, Z.Y. Li, H.M. Huang, F. Yang,W. Zheng, C.Wang, *Mater. Lett.* **61**, 2556 (2007).
22. Xiaojing Shi, Xin Chen, Xiliang Chen, Shaomin Zhou, Shiyun Lou, Yongqiang Wang, Lin Yuan, *Chem. Engineering Journal* **222**, 120–127 (2013).

Proceedings of the 1st African International Conference/Workshop on Applications of Nanotechnology to Energy, Health and Environment, UNN, March 23 – 29, 2014

Page 81